CALCULATING FUSE PRE-ARCING TIMES BY TRANSMISSION-LINE MODELLING (TLM)

L.A.V. Cheim
CEPEL
Rio de Janeiro, Brazil

A.F. Howe
University of Nottingham
Nottingham, U.K.

Abstract

This paper describes a simple, explicit and unconditionally stable routine, based on Transmission-Line Modelling, for the solution of heat diffusion, to calculate electric fuses operating times. Using the technique it was possible to compute fuse pre-arcing times, at low current, and establish good correlation with practical results.

List of principal symbols

T = temperature [K]
H = magnetic field [A/m]
V = electric potential [V]
V^i = incident potential (wave)
V^r = reflected potential (wave)
i = electric current (A)
R_d = electrical resistance per unit length [Ω/m]
R_e = electrical resistance [Ω]
R_x, R_y, R_z = thermal resistance in the direction [K/W]
R_o = electrical resistance at 293.2 K
C_d = capacitance per unit length [F/m]
L_d = inductance per unit length [H/m]
Z = transmission-line impedance [Ω]
$\Delta\ell$ = mesh size in 1-D [m]
σ = electrical conductivity [1/Ωm]
ϵ = electrical permittivity [F/m]
μ = magnetic permeability [H/m]
ρ = density [Kg/m^3]
c_p = specific heat [J/KgK]
k = thermal conductivity [W/mK]

1. Introduction

Transmission Line Modelling (TLM) has been used in a wide variety of applications, including heat transfer, and has proved to be very efficient and often faster than other methods (e.g. Finite Differences).

It is an unconditionally stable technique which means that there is no convergence process for each numerical iteration. Variable meshing and non-uniformity of physical parameters can be easily considered with little extra computation.

It is, therefore, an ideal tool for determining the full range of fuse operating times which may vary from fractions of milliseconds to several hours.

2. Fundamentals of TLM

Although the TLM method was originally designed to analyse electromagnetic problems [1,2] its versatility was soon recognised and the technique was expanded to deal with other problems, including heat transfer [3,4].

Before it is possible to explain how TLM can be applied to analyse the heat diffusion process in electric fuses it is worth considering the fundamentals of the technique, which are summarised in the following sections.

2.1 Diffusion equation

The differential equation which models the potential for the network shown in Fig. 1a is

$$\frac{\partial^2 V}{\partial x^2} = R_d C_d \frac{\partial V}{\partial t} + L_d C_d \frac{\partial^2 V}{\partial t^2} \qquad (1)$$

and for the 3-D network shown in Fig. 1b is

$$\nabla^2 V = 3R_d C_d \frac{\partial V}{\partial t} + 3L_d C_d \frac{\partial^2 V}{\partial t^2} \qquad (2)$$

Maxwell's curl equation for the lossy-wave in a 3-D space is

$$\nabla^2 H = \mu\sigma \frac{\partial H}{\partial t} + \mu\epsilon \frac{\partial^2 H}{\partial t^2} \qquad (3)$$

In the case of diffusion $\mu\sigma >> \mu\epsilon$ so Eq. (3) becomes

$$\nabla^2 H = \mu\sigma \frac{\partial H}{\partial t} \qquad (4)$$

The analogy for the electrical network is that $R_dC_d >> L_dC_d$ which means that the second term in Eq. (2) may be neglected i.e.

$$\nabla^2 V = 3R_d C_d \frac{\partial V}{\partial t} \qquad (5)$$

Because of the similarity of the last two equations it can be inferred that the potential V in the electrical network shown in Fig. 1 has a wave-like behaviour and hence it can be represented by a travelling wave in a lossy transmission line.

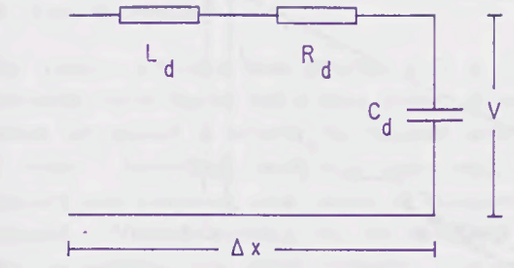

(a) One dimension LRC network

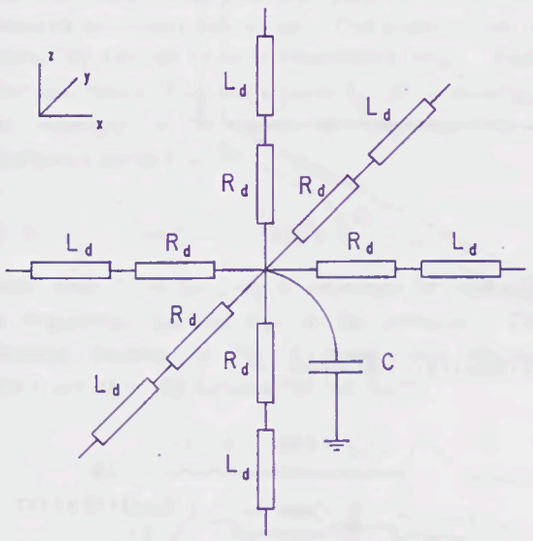

(b) Three dimension LRC network

Fig. 1

2.2 Thermal analogue

The Heat Conduction Equation in Cartesian co-ordinates for a 3-D problem is

$$\nabla^2 T = \frac{c_p \rho}{k} \frac{\partial T}{\partial t} \qquad (6)$$

There is an obvious analogy between Eqs. (5) and (6) provided that

$$3R_d C_d = \frac{c_p \rho}{k} \qquad (7)$$

or

$$\left.\begin{aligned} R_d &= 1/k \\ 3C_d &= c_p \rho \end{aligned}\right] \qquad (8)$$

The similarity between Eqs. (5) and (6) leads to the conclusion that the solution of the wave equation (5) yields the temperature distribution in a 3-D space provided that the specific heat is represented by the capacitances, and the thermal conductivity by the resistances of the network (i.e. node voltages in the TLM model represent point temperatures).

2.3 Transmission-line modelling (TLM)

The medium to be modelled is divided into a number of interconnected elemental transmission-lines - space discretization. Time is also discretized into steps of Δt, the wave transit time for the transmission-line. The impedance Z of the transmission-line can be calculated as

$$Z = \Delta l / C \qquad (9)$$

where

$$C = c_p \rho \Delta x \Delta y \Delta z / 3 \qquad (10)$$

for the 3-D model shown in Fig. 2,

$$Z = 3 \Delta l / c_p \rho \Delta x \Delta y \Delta z \qquad (11)$$

In principle Δt is an arbitrary value, but one should keep in mind that as the whole transmission-line is represented solely by its capacitive component, there is an indictive error L_e. This error is defined by

$$L_e = \Delta l^2 / C \qquad (12)$$

which gets smaller as Δt decreases.
The medium wave velocity is

$$v_m = 1 / \sqrt{LC} \qquad (13)$$

and the TLM wave velocity is

$$V_{TLM} = \Delta l / \Delta t \qquad (14)$$

which shows that the chosen values for $\Delta \ell$ and Δt have to be compromises.
The basic wave equation for the potential at any termination of the transmission-line is

$$V = V^i + V^r \qquad (15)$$

So for the Thevenin equivalent of the network shown in Fig. 2

$$V = \frac{1}{3} \sum_{k=1}^{6} V_k^i \qquad (16)$$

Incident voltage waves will flow along all six branches of the network towards the node, where they will be reflected back, producing corresponding reflected voltages equal to

$$V^r = \frac{R - Z}{R + Z} V^i \qquad (17)$$

Expressing Eqs (15), (16) and (17) for the six branches, one has

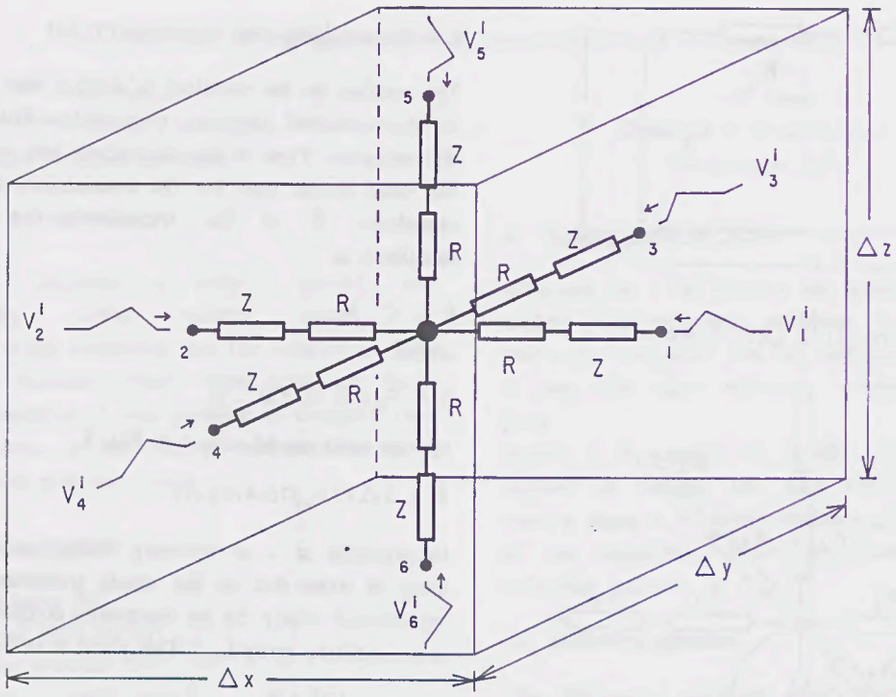

Fig. 2 Three dimension elemental TLM node

$$\begin{vmatrix} V_1^r \\ \cdot \\ \cdot \\ V_6^r \end{vmatrix} = S \cdot \begin{vmatrix} V_1^i \\ \cdot \\ \cdot \\ V_6^i \end{vmatrix} \qquad (18)$$

where

$$S = \frac{1}{3}\begin{vmatrix} -2 & 1 & 1 & 1 & 1 & 1 \\ 1 & -2 & 1 & 1 & 1 & 1 \\ 1 & 1 & -2 & 1 & 1 & 1 \\ 1 & 1 & 1 & -2 & 1 & 1 \\ 1 & 1 & 1 & 1 & -2 & 1 \\ 1 & 1 & 1 & 1 & 1 & -2 \end{vmatrix} \qquad (19)$$

For the first time step all the incident waves are known (initial condition) and from Eq (16) all the potentials at the centre of the node can be calculated. Using the scattering equation (18) all the reflected waves can be determined. This completes the calculation for the actual time step.

For the next iteration each node has to be connected to its neighbour and its 'new' incident wave is set equal to the reflected wave from its neighbour, calculated at the previous iteration (as illustrated in Fig. 3).

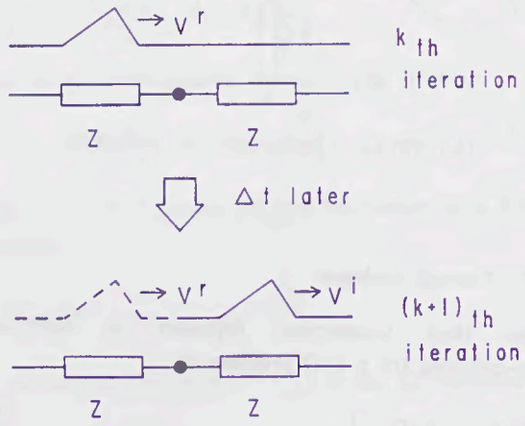

Fig. 3 Connection of two adjacent nodes

Put mathematically,

$$\begin{vmatrix} V^i_{x+1,y} \end{vmatrix} = \begin{vmatrix} V^r_{x,y} \end{vmatrix} \qquad (20)$$

(k+1)th iteration kth iteration

As the new V^i are known all values of V can be computed. The process continues step by step until an artificial time limit is achieved. Boundaries can be dealt with by choosing appropriate line terminations.

2.4 Variable meshing

Most realistic problems have complex 2-D or 3-D geometries which implies that a large number of small meshes are needed to achieve the required accuracy of results. Accordingly small time steps would be necessary and computing time would be substantially increased. Variable meshing can be introduced in order to minimize this effect. However, meshes of variable sizes have different wave impedances and different transit times (see Eq. (11)). These create undesired internodal reflections. This problem can be avoided by the use of stub transmission lines. These stubs are 'extra' lines terminated by an open-circuit and connected to the centre of the node with a capacitance defined by

$$C_{STUB} = C_{node\ A} - C_{node\ B} \qquad (21)$$

where 'node A' is the node of reference for balancing the impedances for the rest of the network. The schematic diagram of Fig. 4 shows what happens before and after the inclusion of the stubs.

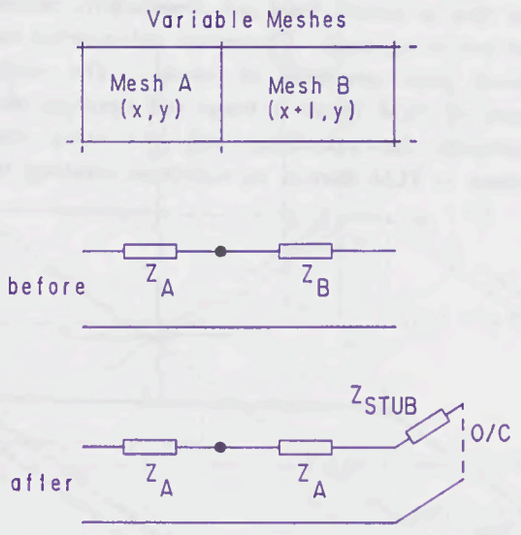

Fig. 4 Effect of adding STUBS to the node

Provided that Eq. (16) is re-defined as

$$V = \frac{\frac{2}{R_x + Z}(V_1^i + V_2^i) + \frac{2}{R_y + Z}(V_3^i + V_4^i) + \frac{2}{R_z + Z}(V_5^i + V_6^i) + \frac{2V_{STUB}}{Z_{STUB}}}{\frac{2}{R_x + Z} + \frac{2}{R_y + Z} + \frac{2}{R_z + Z} + \frac{1}{Z_{STUB}}} \qquad (22)$$

then all the above remains valid.

2.5 Variable parameters

The method of using stubs will also allow for variations in the physical 'constants' of the material which alter the impedance of the transmission-line. So, in the case of the thermal model where c_p and k vary, it will be necessary to adjust the line impedances.

2.6 Electrical analogue

Prior to the TLM calculation it was necessary to know the elemental current for each node. It was assumed that each node had the electrical resistance R_e defined by

$$R = R_0 (1 + \alpha \Delta T) \qquad (23)$$

and that the individual resistances were connected as shown in Fig. 5. The elemental currents, and resistances, were updated as temperature increased every time step.

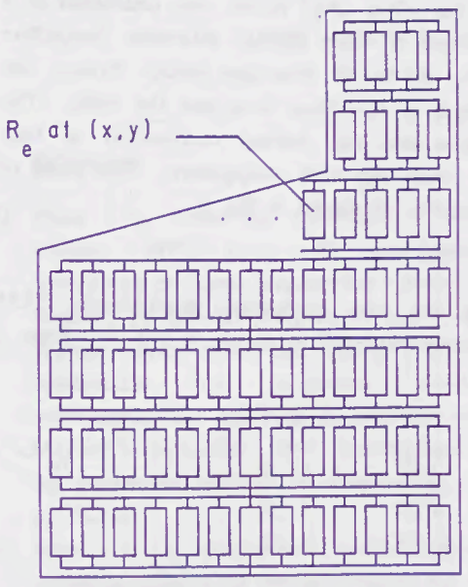

Fig. 5 Parallel-series connection of the electrical resistances of the nodes

2.7 Power source

At each time step the amount of energy ΔE dissipated in the node shown in Fig. 2, due to the elemental current ,i, is given by

$$\Delta E = R_e i^2 \Delta t \qquad (24)$$

This energy will cause a rise in temperature of the node.

The internal energy of the node associated with a variation in temperature ΔT is defined by

$$\Delta U = c_p \rho \Delta x \Delta y \Delta z \Delta T \qquad (25)$$

Assuming that all the energy dissipated in the node is used to increase its internal energy, then $\Delta E = \Delta U$ and hence the temperature rise is equal to

$$\Delta T = \frac{R i^2 \Delta t}{c_p \rho \Delta x \Delta y \Delta z} \qquad (26)$$

3. Modelling of an industrial fuse

To show how TLM can be employed to model practical fuses, the design illustrated in Fig. 6 was chosen. The silver (Ag) ribbon was embedded in a compact block of silica (SiO_2), with heat conduction assumed to be in all directions except through the narrow edges of the silver strip into the silica. The specific heat and the thermal conductivity of both silica and silver vary with temperature. The limits of these variations are shown in Fig. 6.

3.1 Heat dissipation

To allow for heat conduction longitudinally TLM meshes were connected as shown in Fig. 7. Ports 5 and 6 for each metallic node were terminated by the thermal resistance of the silica block immediately above or below.

When 100 A flowed through the fuse illustrated in Fig. 6 the temperature distribution in the metallic strip was found to be as shown in Fig. 8.

3.2 Fuse pre-arcing time × current characteristic

To demonstrate the reliability of TLM to determine the fuse pre-arcing time × current characteristic a number of simulations were done for the fuse illustrated in Fig. 6. The results over the time range 10^{-2} to 10^{1} seconds are presented in Fig. 9. The corresponding computing times varied from a few seconds to 3½ hours. Had it been permitted to run the program for longer periods the simulated characteristic could have been extended, since TLM does not require a convergence process and is explicitly stable.

4. Conclusion

It has been demonstrated that using TLM and an orthogonal, irregular mesh, it is possible to model heat flow in electric fuses and consequently, calculate fuse pre-arcing times. Comparison with practical tests showed good correlation of results. The explicit nature of TLM makes it faster and therefore more convenient for calculating long pre-arcing times because in TLM there is no calculation involving two

	273 K	1254 K
c_p Ag	0.23	0.28
k Ag	4.27	3.55
c_p SiO_2	0.18	0.28
k SiO_2	1.4E-3	4.3E-3

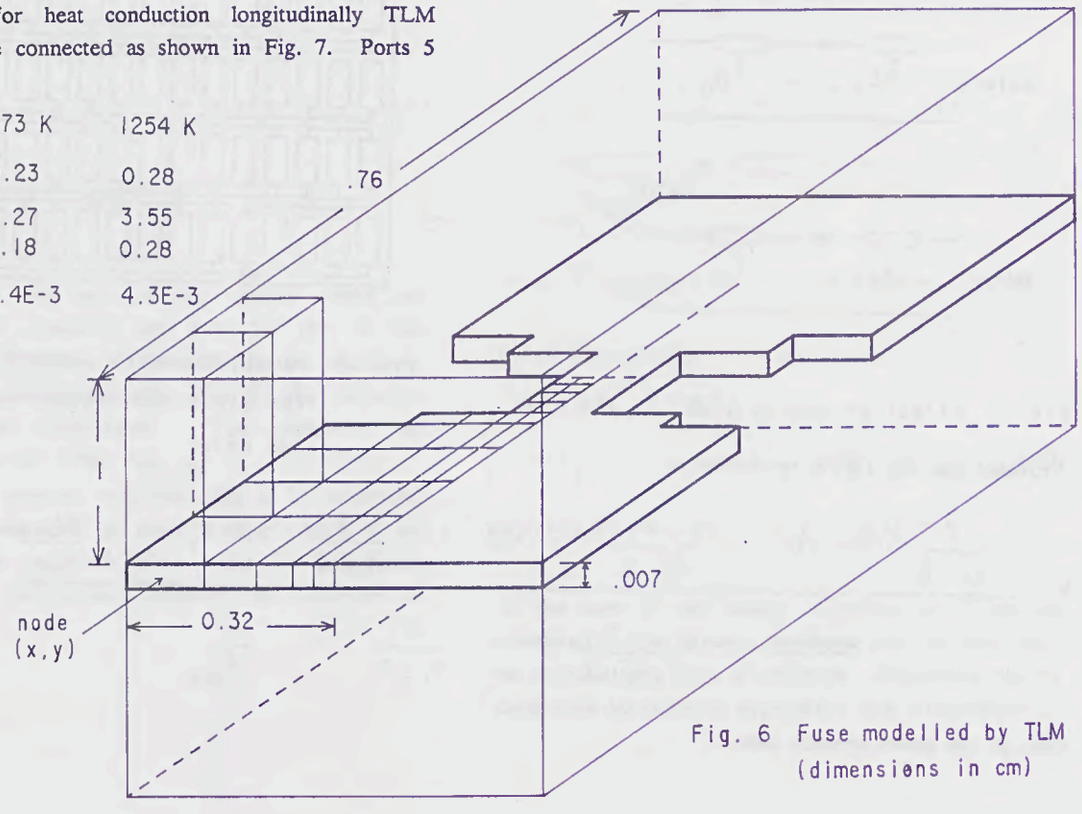

Fig. 6 Fuse modelled by TLM (dimensions in cm)

adjacent nodes for the same time step (unlike Finite Differences where a set of simultaneous linear equations has to be solved each iteration). Although in this work the granular silica was represented by a simple resistor connected to the external ports of the node, this representation could be refined but it would increase computing time. TLM provides a useful tool for the determination of long-time fuse operating characteristics.

5. Acknowledgements

Mr. Cheim wishes to thank the Brazilian Government (CEPEL/CNP$_q$) for its financial support to allow him to study at the University of Nottingham, where he carried out this research in collaboration with Dr. Howe. Both authors are grateful to the University for providing the appropriate facilities.

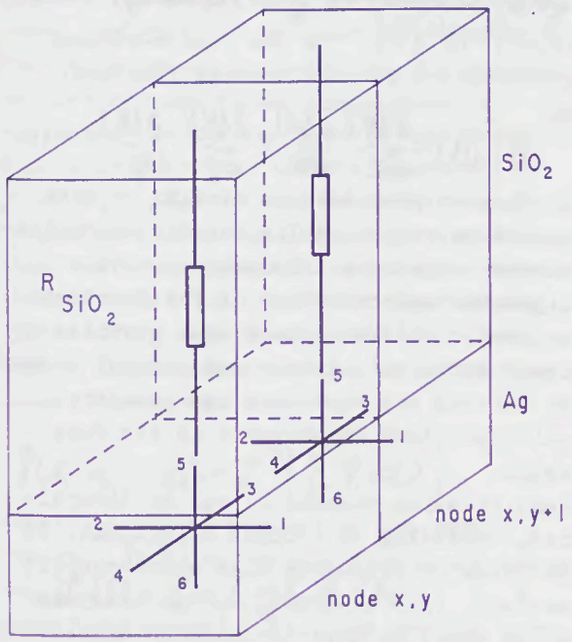

Fig. 7 Metallic nodes and their boundaries

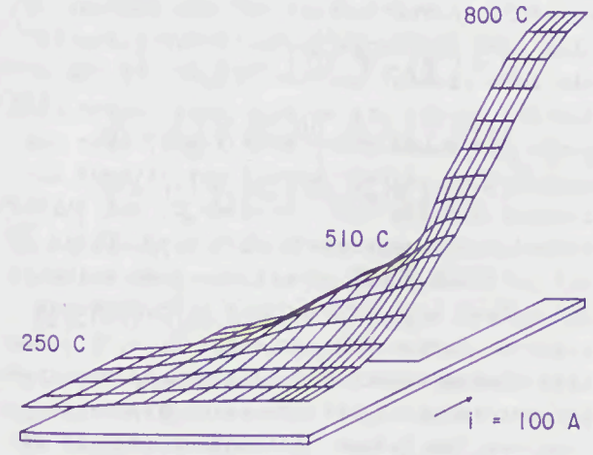

Fig. 8 Temperature profile (3-D) obtained by TLM for the fuse illustrated in Fig. 6

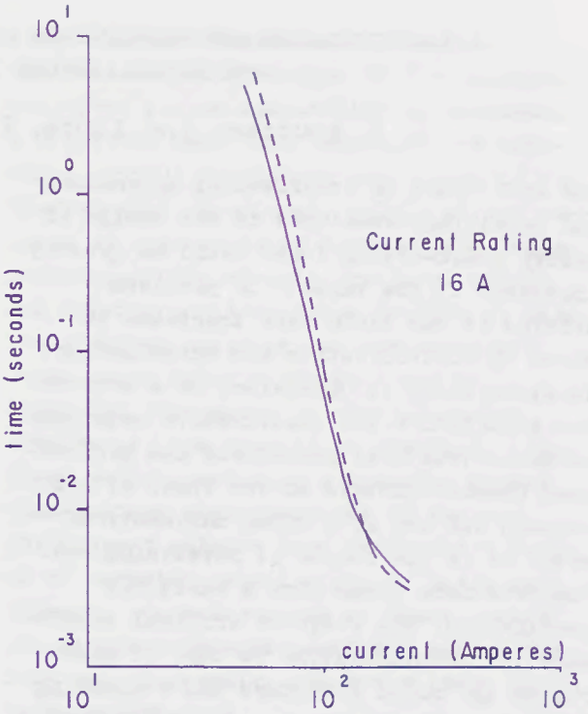

Fig. 9 Time x current characteristics

-- practical results
— TLM simulation

6. References

[1] Johns P.B., Numerical modelling by the TLM method, 1977, Proc. of the International Symposium on Large Engineering Systems (Ed. A. Wexler), pp 139-151 (Pergamon Press, Oxford).

[2] Brewitt-Taylor C.R. and Johns P.B., On the construction and numerical solution of transmission-line and lumped network models of Maxwell's equations, 1980, International Journal for Numerical Methods in Engineering, Vol. 15, pp 13-30.

[3] Johns P.B., A Simple and unconditionally stable numerical routine for the solution of the diffusion equation, 1977, International Journal for Numerical Methods in Engineering, Vol. 11, pp 1307-1328.

[4] Pulko S., Mallik A. and Johns P.B., Application of transmission-line modelling (TLM) to thermal diffusion in bodies of complex geometry, 1986, International Journal for Numerical Methods in Engineering, Vol. 11, pp 2303-2312.

[5] Cook N., TLM Modelling of semiconductor fuses (A feasibility study), 1986, MSc thesis, Nottingham University.

[6] De Cogan D. and Henini M., TLM Modelling of thin film fuses on silica and alumina, 1987, Third International Conference on Electric Fuses and their Applications (ICEFA), Eindhoven, Netherlands, pp 12-17.